Pb EXAFS Studies on DNA Quadruplexes: Identification of Metal Ion Binding Site†

Ivan V. Smirnov,‡ Frank W. Kotch,§ Ingrid J. Pickering,|| Jeffery T. Davis,§ and Richard H. Shafer*,‡

Department of Pharmaceutical Chemistry, School of Pharmacy, University of California, San Francisco, California 94143-0446, Department of Chemistry and Biochemistry, University of Maryland, College Park, Maryland 20742, and Stanford Synchrotron Radiation Laboratory, SLAC, 2575 Sand Hill Road, MS69, Menlo Park, California 94025

Received April 25, 2002

ABSTRACT: Nucleic acid quadruplexes are composed of guanine quartets stabilized by specific metal ions. X-ray diffraction can provide high-resolution information on the structure and metal binding properties of quadruplexes, but only if they can be crystallized. NMR can provide detailed information on the solution structure of such quadruplexes but little quantitative data concerning the metal binding site. Here we apply extended X-ray absorption fine structure (EXAFS) measurements to characterize the metal ion binding site, in frozen solution, of the unimolecular quadruplex formed by the thrombin binding aptamer, d($G_2T_2G_2TGTG_2T_2G_2$) (**TBA**), in the presence of Pb^{2+} ions. The Pb L_{III} -edge X-ray absorption spectrum of this metal−DNA complex is very similar to that we obtain for a Pb^{2+}-stabilized quartet system of known structure constructed from a modified guanine nucleoside (**G1**). The Fourier transforms of the Pb^{2+} complexes with both **TBA** and **G1** show a first-shell interaction at about 2.6 Å, and a weaker, broader shell at 3.5−4.0 Å. Quantitative analysis of the EXAFS data reveals the following: (i) very close agreement between interatomic distances at the metal coordination site for the Pb^{2+}−**G1** complex determined by EXAFS and by X-ray crystallography; (ii) similarly close agreement between interatomic distances measured by EXAFS for the Pb^{2+}−**G1** and Pb^{2+}−**TBA** complexes. These results provide strong evidence for binding of the Pb^{2+} ion in the region between the two quartets in the Pb^{2+}−**TBA** complex, coordinated to the eight surrounding guanine O6 atoms. The specific binding of Pb^{2+} to DNA examined here may be relevant to the genotoxic effects of this environmentally important heavy metal. Furthermore, these results demonstrate the utility of EXAFS as a method for quantitative characterization of specific metal binding sites in nucleic acids in solution.

Metal ion−DNA interactions are important in nature, often impacting the genetic material's structure and function. To better understand the molecular details of these interactions, it is essential that we have a reliable picture of the metal ion coordination site. This is not always so straightforward. Thus, X-ray diffraction can provide high-resolution information on the structure and metal binding properties of nucleic acids, but only if diffraction-quality crystals can be obtained. NMR can provide detailed information on solution structure, but usually little quantitative data concerning the metal binding site. This paper describes how extended X-ray absorption fine structure (EXAFS)[1] measurements can be used to gain detailed information about a Pb^{2+} binding site within a folded DNA oligonucleotide.

DNA and RNA can form quadruplex structures in the presence of certain metal ions, based on the guanine quartet, which is shown in Figure 1A. Only a small number of X-ray crystal structure determinations on quadruplexes have been reported, and these have located the metal binding site in the region between two quartet stacks, or coplanar with one of the quartets (*1*−*3*). There have been numerous NMR solution structural studies of quadruplexes that have delineated the overall fold of the nucleic acid strands and the detailed nucleic acid conformation (*4*−*6*). In most cases, little direct information concerning the location of the stabilizing cation is available from such studies. One exception is the recent report identifying the location of bound NH_4^+ cations between adjacent quartets in the $[d(G_4T_4G_4)]_2$ quadruplex, via cation−DNA ^{1}H-^{1}H NOE's (*7*). This approach, however, is not readily extended to metal ions. More recently, solid-state ^{23}Na NMR techniques have been exploited to characterize the number and type of bound metal ions in the $[d(TG_4T)]_4$ quadruplex (*8*), although quantitative distance information was not available.

† Supported by NIH Grant AI39152, grants from the UCSF Academic Senate and from the UC Toxic Substances Research and Training Program, and a grant from the Separations and Analysis Program, Basic Energy Sciences, U.S. Department of Energy. Portions of this research were carried out at the Stanford Synchrotron Radiation Laboratory, a national user facility operated by Stanford University on behalf of the U.S. Department of Energy, Office of Basic Energy Sciences. The SSRL Structural Molecular Biology Program is supported by the Department of Energy, Office of Biological and Environmental Research, and by the National Institutes of Health, National Center for Research Resources, Biomedical Technology Program.

* To whom correspondence should be addressed. Email: shafer@cgl.uscf.edu.

‡ University of California, San Francisco.

§ University of Maryland.

|| Stanford Synchrotron Radiation Laboratory.

[1] Abbreviation: EXAFS, extended X-ray absorption fine structure.

10.1021/bi020310p CCC: $22.00
Published on Web 09/07/2002

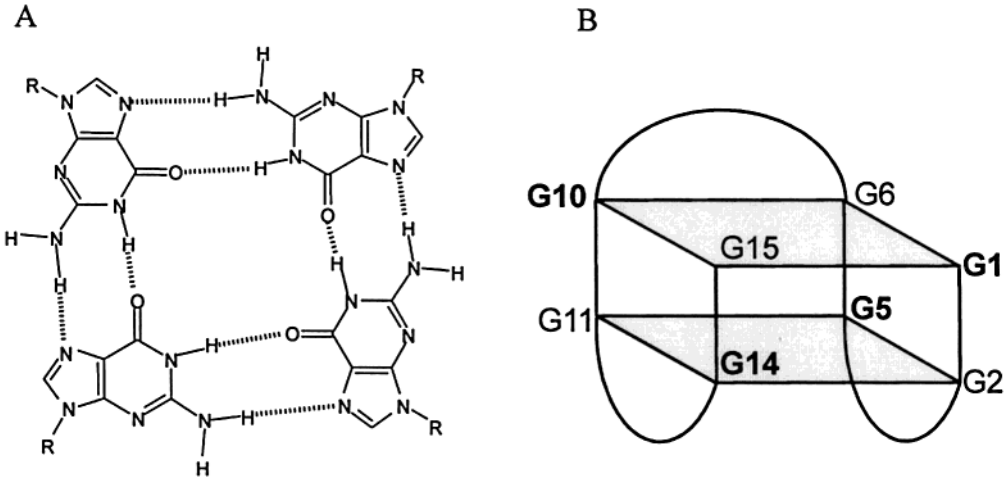

FIGURE 1: (A) Structure of the guanine quartet; (B) schematic drawing of the folded aptamer **TBA**, d($G_2T_2G_2TGTG_2T_2G_2$). Shaded regions represent guanine quartets. Boldface denotes nucleosides in *syn* conformation.

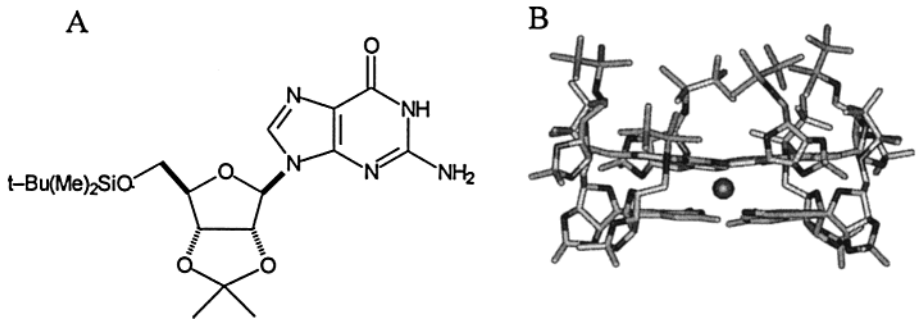

FIGURE 2: (A) Structure of lipophilic guanosine analogue **G1**; (B) view of two quartets with a coordinated Pb^{2+} ion (sphere) from the crystal structure of the Pb^{2+}−**G1** complex (*17*).

Other metal nuclei have been studied by NMR. ^{205}Tl NMR, for example, has been exploited to characterize the bound Tl^+ cations used to stabilize the $[d(T_2G_4T_2)]_4$ quadruplex (*9*). Likewise, ^{207}Pb NMR can be used to examine the Pb^{2+} ion bound to quadruplex structures (*10*). As in the case of the ^{23}Na NMR studies, NMR spectra of these other metal nuclei can help delineate the number and type of bound metal ions, but quantitative distances between the metal and the nucleic acid are difficult to determine. It is thus apparent that a method suitable for quantitatively characterizing metal coordination sites in nucleic acids in the solution phase would be very useful. Below we show that EXAFS is one such method, which, in combination with other methods, such as CD and NMR, can determine the geometry of a metal binding domain in a Pb^{2+}-stabilized folded guanine quadruplex.

The thrombin binding aptamer (**TBA**) is a 15-mer DNA oligonucleotide which, in the presence of K^+, folds into a unimolecular quadruplex consisting of two quartets connected by three loops (*11*, *12*), shown schematically in Figure 1B. Previously, we reported that Pb^{2+} is highly effective at folding **TBA** at a 1:1 metal:strand stoichiometry and that its conformation is qualitatively similar to that obtained when folded by potassium (*13*). Several important differences were noted between the Pb^{2+}−**TBA** and K^+−**TBA** complexes: (i) binding of the divalent cation was much tighter than that of the monovalent cation; (ii) a single Pb^{2+} ion sufficed to fully fold the aptamer compared to two K^+ ions (*14*); (iii) the positive peak in the CD spectrum of the Pb^{2+} complex was centered at 312 nm, corresponding to a bathochromic shift of almost 20 nm in comparison to that of the K^+ complex. In a computational analysis based on the solution conformation of **TBA** in KCl determined by ^1H NMR, Bolton and co-workers proposed that the tight binding site for K^+ is located outside the inter-quartet region (*14*, *15*).

Here we show how extended X-ray absorption fine structure (EXAFS) studies on metal−DNA complexes, in conjunction with similar studies on model guanine quartets of known structure, composed of the lipophilic guanosine nucleoside **G1** (see Figure 2A) (*16*, *17*) can be used to investigate the DNA metal binding site. In particular, using this approach we identify the Pb^{2+} ion binding site in the region between the two quartets in **TBA** and obtain quantitative distances between the metal ion and the surrounding nucleic acid atoms. This study also illustrates how a biomimetic model system can provide considerable insight into biomolecular structure. To date, we have studied **G1** mostly in the context of supramolecular chemistry, examining its ability to self-assemble in organic solvents to serve as a noncovalent ionophore. In addition, **G1** self-assembles to give a lipophilic G-quadruplex that has many of the structural features exhibited by DNA G-quadruplexes (*16*, *17*). Thus, the nucleoside analogue **G1** has much promise as a useful model system for gaining information about more biologically relevant compounds. Indeed, recent NMR studies on this model guanosine compound have already demonstrated its usefulness in understanding structural studies on guanine quadruplex structures (*18*).

MATERIALS AND METHODS

DNA sequences d($G_2T_2G_2TGTG_2T_2G_2$) (**TBA**), d($G_2A_2G_2$-$TGTG_2A_2G_2$) (**TBAA**), and d(GCGA_2T_2CGC) (**DUP**) were purchased from OligosEtc, and stock solutions were made up in 10 mM Tris−acetate, pH 6.8. Purity was estimated to be in the range of at least 90−95% as determined by polyacrylamide gel electrophoresis. The lipophilic nucleoside **G1** was synthesized as described previously (*17*), extracted with an aqueous solution of Pb(picrate)$_2$, crystallized from acetonitrile−methylene chloride, and then redissolved in $CDCl_3$. Its purity was checked by both ^{1}H and ^{207}Pb NMR.

Samples were prepared for EXAFS measurements as follows. Aqueous samples of **TBA**, **TBAA**, and **DUP** complexed with Pb^{2+} were made up in 10 mM Tris−acetate buffer, pH 6.8, by addition of $Pb(NO_3)_2$. The metal concentration was 5−6 mM in the presence of ∼20% excess DNA strand in a volume of 150 μL. The sample was heated to 90 °C for 5 min and then cooled to room temperature. Quadruplex formation in the presence of Pb^{2+} was confirmed by CD. The sample was added to a Lucite cell with lead-free Mylar or Kapton tape windows, flash-frozen in a mixture of 2-methylbutane and liquid nitrogen, and held in liquid nitrogen until placed in the beam line for measurement. The lipophilic guanosine nucleoside **G1** complexed with Pb^{2+} was isolated as a solid powder by slow evaporation of $CDCl_3$, subjected to gentle grinding, and placed in a Teflon sample cell.

Pb L_{III}-edge X-ray absorption spectra were measured on beamline 7-3 at the Stanford Synchrotron Radiation Laboratory using a Si(220) double-crystal monochromator with an upstream vertical aperture of 1 mm. No focusing optics were present in the beamline, and harmonic rejection was accomplished by detuning one crystal off-peak to give 50% intensity. The SPEAR storage ring was operating at 3 GeV, and ring currents were in the range 50−100 mA. Data were recorded both in the transmission mode using nitrogen-filled chambers and in the fluorescence mode, with either a Canberra 13-element or a 30-element germanium detector. Typically, data from 4−10 scans were collected for each sample. X-ray energy calibration was achieved by simultaneous measurement of the absorption of a Pb foil. The first inflection point of the foil absorption edge was taken to be 13 038 eV. Samples were maintained at temperatures close to 10 K in an Oxford Instruments flowing liquid helium cryostat.

All data processing and fitting were carried out using the program EXAFSPAK (www-ssrl.slac.Stanford.edu/exafspak.html). Data from multiple scans and, in the case of fluorescence, multiple channels were averaged and normalized by incident intensity, I_0. The EXAFS spectrum, $\chi(k)$, was extracted from the data by preedge subtraction, spline subtraction, and Victoreen normalization; in some cases, monochromator crystal glitches were removed as well. The resulting function was then weighted by k^3 and fitted using ab initio phases and amplitudes calculated using the program Feff8 (*19*). The coordinates for a representative lead site from the Pb^{2+}−**G1** model structure were used in the calculation. The paths generated were examined for significance, and four types were found to be necessary to fit the substantial features of the spectrum, below about 4 Å. The first shell consisted of eight Pb−O at about 2.6 Å. The second shell involved two single scattering (two-leg) paths, eight Pb···C at 3.6 Å and eight Pb···N at 3.9 Å, together with a three-leg path, Pb−O−C−Pb, at about 3.7 Å and with a multiplicity of 16. A representative path from each of these types was chosen, and the phase, amplitude, and mean free path functions were used in the refinements.

The nominal energy threshold value was set to 13 055 eV, and an offset to this value (ΔE_0) was refined during analysis. The Pb^{2+}−**G1** model data were fit first with the coordination numbers (N) fixed according to the known structure (*17*) and refining distances (R), Debye−Waller factors (σ^2), the scale factor, and ΔE_0. As the σ^2 for the various shells refined to very similar values, in subsequent fits they were constrained to be the same value and were floated as a single variable, to reduce correlations. In the next fit, a common second-shell N parameter was floated (the three coordination numbers were constrained to maintain the ratio 8:16:8 for Pb···C, Pb−O−C−Pb, and Pb···N, respectively, and floated as a single parameter) together with all distances, the common σ^2, the scale factor, and ΔE_0. The scale factor and ΔE_0 were fixed at the values thus obtained (1.08 and −3.54 eV, respectively). Subsequently, for each data set, the first- and second-shell N values, the four distances, and the common σ^2 were floated.

RESULTS AND DISCUSSION

The Pb L_{III} EXAFS oscillations for the Pb^{2+}−**TBA** and Pb^{2+}−**TBAA** complexes are presented in Figure 3A, along with those for the model compound, Pb^{2+}−**G1**. All three EXAFS spectra are very similar, signifying a similar environment surrounding the metal ion in these structures. The corresponding Fourier transforms for these three systems are presented in Figure 3B. Again, results for all three guanine quartet systems are comparable, with a major first-shell peak at ∼2.6 Å and a smaller, broader peak centered around ∼3.7 Å. EXAFS data were also collected on a nonquadruplex DNA system, the double helix form of the self-complementary decamer **DUP** in the presence of Pb^{2+}. This Pb^{2+}−duplex system exhibits a very different EXAFS spectrum, with substantially lower amplitude which decreases much more quickly with increasing k than those of the quadruplex structures (Figure 3A). This behavior is characteristic of a less ordered environment for the metal ion. Fourier transform of this EXAFS spectrum (Figure 3B) reveals a single peak near 2.5 Å, much smaller than the first shells of the other spectra, with no peaks at larger distances from the metal. Similarly, the near-edge spectra are also quite distinct for the Pb^{2+}−duplex complex compared to the quartet-based structures, as illustrated in Figure 4.

To facilitate detailed analysis of the EXAFS data on the aptamer metal complexes, we first investigated quantitatively the Pb^{2+}−**G1** complex as a model for the Pb^{2+} environment postulated for the DNA complexes. Multiple scattering analysis of the EXAFS data for the Pb^{2+}−**G1** system, in conjunction with the known crystal structure illustrated in Figure 2B (*17*), employed three shells of atoms surrounding the metal. The first, located at 2.65 Å, corresponds to the eight O6 atoms, one from each guanine in both quartets surrounding the metal ion. The second and third shells appear at 3.59 and 3.93 Å, too close together to be resolved in the

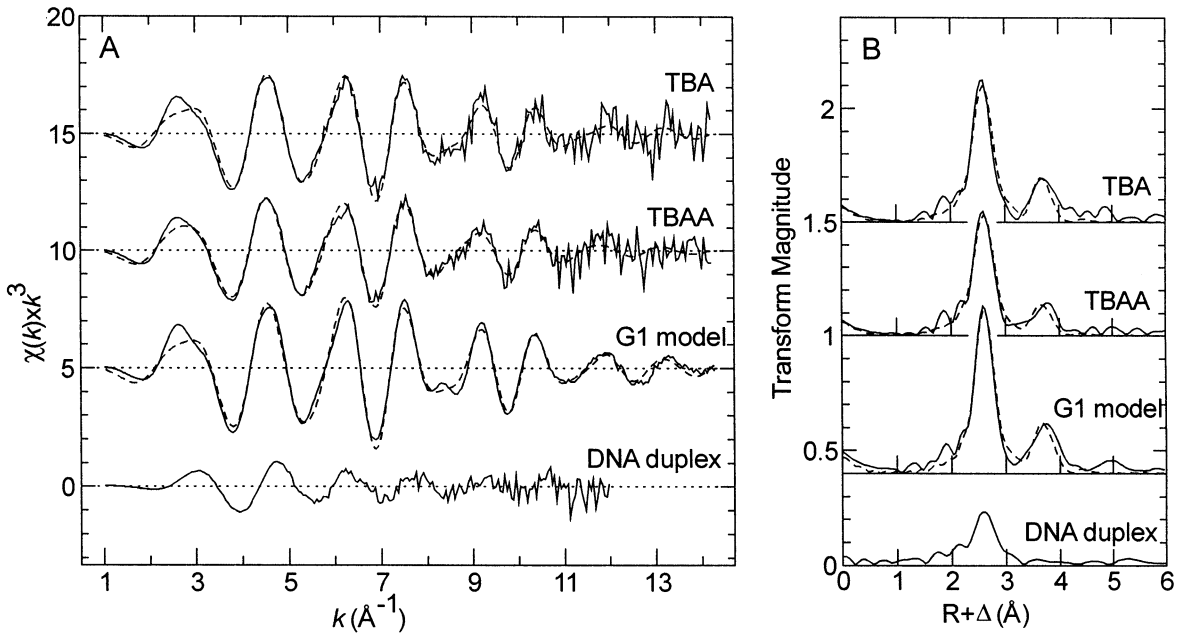

FIGURE 3: Pb L_{III} EXAFS functions (A) and their Fourier transforms (phase-corrected for first shell Pb−O) (B) for the Pb^{2+} complexes with **G1**, **TBA**, **TBAA**, and **DUP**; experiment (—), best fit (- - -). Note that the Fourier transform range for the **DUP** complex is shorter than for the others.

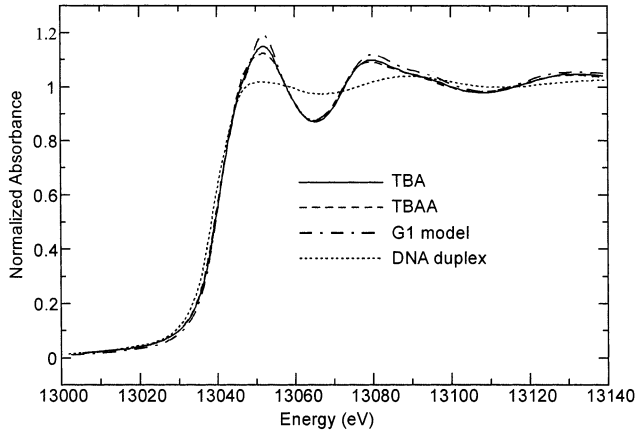

FIGURE 4: Pb L_{III} X-ray absorption near-edge spectrum for the four Pb^{2+} complexes with **G1**, **TBA**, **TBAA**, and **DUP**.

Fourier transform, and correspond to the eight guanine C6 and N1 atoms, respectively. A 3-leg multiple scattering path, corresponding to Pb−O6−C6−Pb, and contributing 4% to the EXAFS, was additionally needed to give an adequate fit. The resulting fits to the EXAFS functions and their Fourier transforms are included in Figure 3. Parameters determined by fitting are summarized in Table 1. Comparison of the mean interatomic distances with those obtained from the X-ray crystal structure, also included in Table 1, indicates agreement between the EXAFS and X-ray diffraction results for the Pb^{2+}−**G1** complex to within ±0.02 Å for the Pb−O shell and to within ±0.04 Å for the Pb···C and Pb···N distances. For all of these shells, the two measurements agree within the standard deviations.

From analysis of the EXAFS function for the Pb^{2+}−**TBA** complex, we obtained coordination numbers of 7.4 for the first shell and 8.1 for the outer shells, as summarized in Table 1. These numbers differ by at most 8% from those of the Pb^{2+}−**G1** complex, well within the expected uncertainty for coordination numbers (*20*), and are the same within the confidence limits of the fit. Additionally, the presence of three shells with similar coordination numbers argues strongly for direct coordination of dehydrated Pb^{2+} ions to the DNA in a highly ordered state. The interatomic distances of 2.64, 3.58, and 3.90 Å obtained for Pb−O, Pb···C, and Pb···N, respectively, are in very close agreement with the distances obtained by EXAFS on the Pb^{2+}−**G1** model system. The slightly lower amplitude of the **TBA** EXAFS (Figure 3A), reflected in a somewhat bigger Debye−Waller factor (Table 1), suggests a slightly elevated static disorder compared with **G1**. This difference in disorder is probably due, at least in part, to the difference in solid and solution preparations of the **G1** and **TBA** complexes.

It is of interest to note that a survey of Pb^{2+} compounds in the Cambridge Crystal Structure Database (*21*) showed that, for Pb coordinated to 8 oxygens, the average Pb−O distance ranged from 2.54 to 2.70 Å (16 different lead sites) with the mean value being 2.65 Å. By contrast, Pb coordinated to 6 oxygens gave an average Pb−O distance of 2.45−2.62 Å (mean 2.55 Å, 19 sites). Hence, our value of 2.64 Å for the Pb−O distance in the Pb^{2+}−**TBA** complex is much more consistent with coordination to 8 rather than 6 oxygens, which further corroborates our assignment of the Pb binding site in the **TBA** complex as being between the two quartets. The qualitative similarity in EXAFS and Fourier transform functions along with the quantitative agreement between the coordination numbers and distances strongly support the conclusion that the metal ion exists in a similar molecular environment in the complexes with **G1** and **TBA**. These conclusions are also supported by the near-edge spectra displayed in Figure 4.

Since the X-ray crystal structure of the Pb^{2+}−**G1** complex shows the metal ion to be sandwiched between a pair of guanine quartets, our EXAFS results then indicate that the metal is similarly located between the two quartets in the Pb^{2+}−**TBA** complex. This contrasts with the proposed strong binding site for K^+ in the K^+−**TBA** complex, located between the two -TT- loops and the adjacent quartet, with

Table 1: Results of Fitting EXAFS Curve-Fitting Analysis[a]

sample	N_{Pb-O}	R_{Pb-O}	$\sigma^{2\,b}$	$N_{Pb\cdots C}$	$R_{Pb\cdots C}$	$R_{Pb\cdots N}{}^{c}$	F^{d}
G1	8.0(5)	2.648(3)	0.0081(3)	8.3(9)	3.59(1)	3.92(1)	0.062
TBA	7.4(9)	2.644(6)	0.0091(14)	8.1(2.0)	3.58(3)	3.90(2)	0.173
TBAA	7.2(9)	2.657(6)	0.0100(12)	6.3(2.0)	3.57(3)	3.90(3)	0.121
G1 (X-ray)[e]	8	2.66 ± 0.05		8	3.63 ± 0.05	3.95 ± 0.06	

[a] Coordination number, N, interatomic distance, R (Å), common Debye−Waller factor, σ^2 (Å^2), and goodness of fit, F. Numbers in parentheses after the values indicate 3 times the estimated standard deviation in the last digit(s) of the value, as derived from the diagonal elements of the covariance matrix. [b] A common Debye−Waller factor was used for all the shells. [c] $N_{Pb\cdots N} = N_{Pb\cdots C}$. [d] $F = \Sigma k^6(\chi_o - \chi_c)^2/N_o$, where χ_o and χ_c are the observed and calculated EXAFS and N_o is the number of points. [e] Coordination numbers and average distances ± standard deviations taken from X-ray crystal structure of the Pb^{2+}−**G1** complex (*17*).

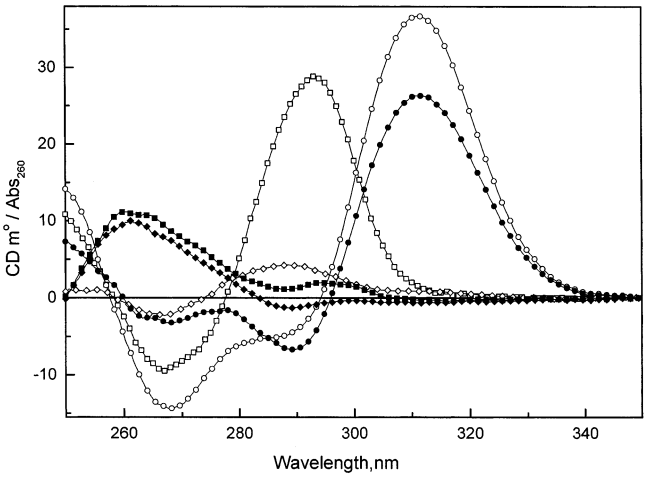

FIGURE 5: CD spectra of aptamers in 10 mM lithium cacodylate, pH 6.8: **TBA** alone (◇), +0.5 mM KCl (□), +10 μM $Pb(NO_3)_2$ (○); **TBAA** alone (◆), +25 mM KCl (■), +50 μM $Pb(NO_3)_2$ (○).

coordination to five or six of the available carbonyl oxygens from the surrounding thymine and guanine bases (*14, 15*). To investigate this difference further, we carried out EXAFS measurements on an analogue of **TBA** in which A replaced all T residues in the two -TT- loops. As can be seen in Figure 5, this sequence, **TBAA**, shows no sign of folding in the presence of KCl, consistent with previous reports that a single A substitution in one of these loops prevents folding in the presence of K^+ (*14*). In the presence of Pb^{2+}, however, **TBAA** folds with little difficulty, exhibiting a CD spectrum similar to that of Pb^{2+}−**TBA**, also illustrated in Figure 5. This difference in folding ability between these two cations, as determined by CD, is consistent with the hypothesis that Pb^{2+} and K^+ may occupy different binding sites when complexed to these quadruplex-forming oligonucleotides. Alternatively, it is possible that both metals bind in the inter-quartet region, with the presence of the bulky purines in the two short loops of **TBAA** resulting in a much more pronounced decrease in affinity for K^+ than for Pb^{2+}.

As shown in Figure 3, the EXAFS spectrum and accompanying Fourier transform measured for the Pb^{2+}−**TBAA** complex are very similar to those determined for the other quartet complexes; the same holds for the near-edge spectra shown in Figure 4. Quantitative analysis of the EXAFS function revealed a set of metal−DNA distances, also included in Table 1, within 0.01 Å of those determined for Pb^{2+}−**TBA**. The coordination numbers determined by this modified aptamer are a little lower than those for the other structures, although within 21% or better, and still within the confidence limits, of the expected value of 8. The observed amplitude of the EXAFS is a little lower than for the unmodified aptamer (Figure 3), and the derived Debye−Waller factor (Table 1) is a little higher. It is possible that the method of fitting we utilized, imposing the same Debye−Waller factors for all shells, may not accurately reflect the relative disorder in the modified aptamer, **TBAA**. The presence of two bulky purines in each of the lateral loops may produce a different distribution of static and/or dynamic disorder compared to the unmodified aptamer. In this regard, we note that the affinity of **TBAA** for Pb^{2+} is approximately 3−5 times lower than that of **TBA**, yet still large enough (i.e., $\sim 10^7$ M^{-1}) such that all the metal is coordinated to the DNA at the concentrations used in our experiments (*13*). Given the well-known correlation between coordination number and Debye−Waller factors, it is not feasible to obtain highly accurate values for both these parameters in fitting data. Within these limitations, our results indicate that Pb^{2+} is able to fold **TBAA** while K^+ cannot, and that the environment surrounding the divalent metal ion is similar in both **TBA** and **TBAA**.

Although the Pb^{2+} complex with **G1** was analyzed in terms of four shells, corresponding to the first two peaks in the Fourier transform, examination of Figure 3B reveals a third, well-resolved small peak for this model compound. This third peak occurs near 4.8 Å, in close agreement with the X-ray crystal structure of the Pb^{2+}−**G1** complex, where the next shell of atoms beyond 4 Å, consisting of a single shell Pb···C and several multiple scattering paths, occurs at 4.79−4.95 Å. This third peak is not apparent in the Pb^{2+}−aptamer complexes, most likely due to the greater disorder characteristic of the solution state and the increased noise in the data.

RNA can also bind Pb^{2+} ions specifically, and several X-ray crystal structures have been reported for tRNA and the leadzyme, for example. In the case of tRNA, several Pb^{2+} binding sites were identified, with one or two direct contacts to RNA (*22, 23*). It was presumed that multiple waters remained coordinated to the metal while complexed to tRNA, although none were located, probably due to limited resolution. Similarly, in the leadzyme structure (*24*), a single Pb^{2+} binding site was directly observed, making two contacts to the RNA. These RNA−metal binding sites differ significantly from the DNA metal site described here, which entails eight inner-sphere contacts of the metal with the nucleic acid and, presumably, a completely dehydrated metal ion.

EXAFS is particularly well suited to characterizing the molecular structure surrounding coordinated metals, and is commonly employed with this goal in mind for metal−protein complexes (*20, 25*). Few examples are available, however, of EXAFS studies in metal−nucleic acid com-

plexes (*26, 27*), primarily due to the relatively weak binding of many metals to nucleic acids, the tendency for metals to bind at phosphate groups, and the prevalence of bound metals retaining many, if not all, of their waters of hydration. Our results on the model compound, Pb^{2+}−**G1**, containing no phosphate groups and crystallized from organic solvents, are therefore of particular significance regarding this point, as the metal cannot be complexed with phosphate oxygens nor can they be hydrated. Furthermore, the presence of outer shells in the Fourier transforms of the EXAFS functions for the aqueous DNA quadruplex samples is additional support for coordination of the dehydrated metal ion to the DNA bases. Only a single shell was observed in our results on the metal in the presence of duplex DNA and indeed may represent the existence of a predominantly hydrated metal ion in that case.

CONCLUSION

In summary, we have shown for the first time that EXAFS can be used to both identify and quantitatively characterize, in solution, metal binding sites in nucleic acids. Our focus on the Pb^{2+}−**TBA** complex was motivated by our recent demonstration of very tight, sequence-specific and stoichiometric binding of this heavy metal to DNA (*13*). Certainly, interaction of Pb^{2+} with genetic material may contribute to its damaging effects in humans, and it is conceivable that lead's genotoxicity may arise from its ability to stabilize folded DNA structures. More generally, this method will be useful for similar investigations on other metal−nucleic acid complexes. For example, divalent metals, such as Sr^{2+} (*13, 28, 29*) and Ba^{2+} (*30, 31*), have been shown to stabilize quadruplexes and are currently under investigation. Of course, it will be of particular interest to examine the K^+−**TBA** complex with EXAFS, although that will be a more difficult experiment due to the low energy of the potassium K-edge. Additionally, Pb^{2+} and other divalent cations are often critically important in catalytic DNA and RNA constructs. Thus, these systems may also be amenable to structural analysis via EXAFS. Finally, we mention that the set of heavy-atom distances between the metal and the nucleic acid determined by EXAFS can be used in conjunction with interproton distances determined by NMR to obtain improved solution structures compared to those determined with interproton distances only.

ACKNOWLEDGMENT

It is a pleasure to thank Dr. Graham George, Stanford Synchrotron Radiation Laboratory, for many helpful discussions, and the SSRL staff for their invaluable assistance.

REFERENCES

1. Kang, C., Zhang, X., Ratliff, R., Moyzis, R., and Rich, A. (1992) Crystal structure of four-stranded *Oxytricha* telomeric DNA. *Nature 356*, 126−131.
2. Phillips, K., Dauter, Z., Murchie, A. I. H., Lilley, D. M. J., and Luisi, B. (1997) The crystal structure of a parallel-stranded guanine tetraplex at 0.95 angstrom resolution. *J. Mol. Biol. 273*, 171−182.
3. Deng, J., Xiong, Y., and Sundaralingam, M. (2001) X-ray analysis of an RNA tetraplex (UGGGGU)(4) with divalent Sr(2+) ions at subatomic resolution (0.61 Å). *Proc. Natl. Acad. Sci. U.S.A. 98*, 13665−13670.
4. Gilbert, D. E., and Feigon, J. (1999) Multistranded DNA structures. *Curr. Opin. Struct. Biol. 9*, 305−314.
5. Feigon, J., Koshlap, K. M., and Smith, F. W. (1995) ^{1}H NMR spectroscopy of DNA triplexes and quadruplexes. *Methods Enzymol. 261*, 225−255.
6. Patel, D. J., Bouaziz, S., Kettani, A., and Wang, Y. (1999) in *Oxford Handbook of Nucleic Acid Structures* (Neidle, S., Ed.) pp 349−453, Oxford University Press, Oxford.
7. Hud, N. V., Schultze, P., Sklenár, V., and Feigon, J. (1999) Binding sites and dynamics of ammonium ions in a telomere repeat DNA quadruplex. *J. Mol. Biol. 285*, 233−243.
8. Rovnyak, D., Baldus, M., Wu, G., Hud, N. V., Feigon, J., and Griffin, R. G. (2000) Localization of Na-23(+) in a DNA quadruplex by high-field solid-state NMR. *J. Am. Chem. Soc. 122*, 11423−11429.
9. Basu, S., Szewczak, A. A., Cocco, M., and Strobel, S. A. (2000) Direct detection of monovalent metal ion binding to a DNA G-quartet by Tl-205 NMR. *J. Am. Chem. Soc. 122*, 3240−3241.
10. Smirnov, I. V., Gochin, M., and Shafer, R. H. (2001), unpublished results.
11. Wang, K. Y., McCurdy, S., Shea, R. G., Swaminathan, S., and Bolton, P. H. (1993) A DNA aptamer which binds to and inhibits thrombin exhibits a new structural motif for DNA. *Biochemistry 32*, 1899−1904.
12. Macaya, R. F., Schultze, P., Smith, F. W., Roe, J. A., and Feigon, J. (1993) Thrombin-binding DNA aptamer forms a unimolecular quadruplex structure in solution. *Proc. Natl. Acad. Sci. U.S.A. 90*, 3745−3749.
13. Smirnov, I., and Shafer, R. H. (2000) Lead is unusually effective in sequence-specific folding of DNA. *J. Mol. Biol. 296*, 1−5.
14. Marathias, V. M., and Bolton, P. H. (1999) Determinants of DNA quadruplex structural type: sequence and potassium binding. *Biochemistry 38*, 4355−4364.
15. Marathias, V. M., and Bolton, P. H. (2000) Structures of the potassium-saturated, 2:1, and intermediate, 1:1, forms of a quadruplex DNA. *Nucleic Acids Res. 28*, 1969−1977.
16. Forman, S. L., Fettinger, J. C., Pieraccini, S., Gottareli, G., and Davis, J. T. (2000) Toward artificial ion channels: A lipophilic G-quadruplex. *J. Am. Chem. Soc. 122*, 4060−4067.
17. Kotch, F. W., Fettinger, J. C., and Davis, J. T. (2000) A lead-filled G-quadruplex: insight into the G-quartet's selectivity for Pb^{2+} over K^+. *Org. Lett. 2*, 3277−3280.
18. Wong, A., Fettinger, J. C., Forman, S. L., Davis, J. T., and Wu, G. (2002) The sodium ions inside a lipophilic G-quadruplex channel as probed by solid-state Na-23 NMR. *J. Am. Chem. Soc. 124*, 742−743.
19. Ankudinov, A. L., Ravel, B., Rehr, J. J., and Conradson, S. D. (1998) Real-space multiple-scattering calculation and interpretation of X-ray-absorption near-edge structure. *Phys. Rev. B: Condens. Matter 58*, 7565−7576.
20. Cramer, S. P. (1988) in *X-ray absorption: principles, applications, techniques of EXAFS, SEXAFS, and XANES* (Koningsberger, D. C., and Prins, R., Eds.) pp 257−320, Wiley, New York.
21. Allen, F. H., and Kennard, O. (1993) *Chem. Des. Autom. News 1*, 31−37.
22. Brown, R. S., Hingerty, B. E., Dewan, J. C., and Klug, A. (1983) Pb(II)-catalysed cleavage of the sugar−phosphate backbone of yeast tRNAPhe—implications for lead toxicity and self-splicing RNA. *Nature 303*, 543−546.
23. Brown, R. S., Dewan, J. C., and Klug, A. (1985) Crystallographic and biochemical investigation of the lead(II)-catalyzed hydrolysis of yeast phenylalanine tRNA. *Biochemistry 24*, 4785−4801.
24. Wedekind, J. E., and McKay, D. B. (1999) Crystal structure of a lead-dependent ribozyme revealing metal binding sites revelant to catalysis. *Nat. Struct. Biol. 6*, 261−268.
25. Scott, R. A. (2000) in *Physical methods in bioinorganic chemistry: spectroscopy and magnetism* (Que, L., Jr., Ed.) pp 465−503, University Science Books, Sausalito, CA.
26. Teo, B. K., Eisenberger, J. R., Barton, J. K., and Lippard, S. J. (1978) Study of the binding of *cis*- and *trans*-dichlorodiammine-platinum(II) to calf thymus DNA by extended X-ray absorption fine structure spectroscopy. *J. Am. Chem. Soc. 100*, 3325−3327.
27. Skuratovskii, I. Y., Hasnain, S. S., Alexeev, D. G., Diakun, G. P., and Volkova, L. I. (1987) EXAFS studies of the calcium salts of natural DNA and polydA:polydT. *J. Inorg. Biochem. 29*, 249−257.
28. Chen, F. M. (1992) Sr^{2+} facilitates intermolecular G-quadruplex formation of telomeric sequences. *Biochemistry 31*, 3769−3776.

29. Shi, X., Fettinger, J. C., and Davis, J. T. (2001) Ion pair recognition via nucleoside self-assembly: guanosine hexadecamers bind cations and anions. *Angew. Chem., Int. Ed. Engl. 40*, 2827−2831.
30. Venczel, E. A., and Sen, D. (1993) Parallel and antiparallel G-DNA structures from a complex telomeric sequence. *Biochemistry 32*, 6220−6228.
31. Shi, X., Fettinger, J. C., and Davis, J. T. (2001) Homochiral G-quadruplexes with Ba^{2+} but not with K^{+}: the cation programs enantiomeric self-recognition. *J. Am. Chem. Soc. 123*, 6738−6739.

BI020310P